The Development of Active Vortex Generators from Shape Memory Alloys for the Convective Cooling of Heated Surfaces

M.S.Aris[a,*], I.Owen[b], C.J.Sutcliffe[b]

[a]Department of Mechanical Engineering, Universiti Teknologi Petronas, Bandar Sri Iskandar, 31750 Perak, Malaysia.
[b]Department of Mechanical Engineering, University of Liverpool, Brownlow Hill, L69 3GH, Liverpool, United Kingdom.

ABSTRACT

A study of the convective heat transfer enhancement of heated surfaces through the use of active delta wing vortex generators is reported in this paper. The surface-mounted vortex generators (VGs) change their shape to intrude further into the flow at high temperatures to enhance heat transfer, while maintaining a low profile at low temperatures to minimise flow pressure losses. The VGs are made from shape memory alloys and manufactured in a selective laser melting process. Experiments have been carried out in a rectangular duct supplied with laminar-transition air flow. In the test section, a single, and a pair of active delta wing VGs were placed near the leading edge of a heated plate and tested separately for their heat transfer enhancement effects using Infrared Thermography. The pressure difference across the test section was also measured to determine the pressure drop penalty associated with the obstruction caused by the vortex generators in their active positions. Promising shape memory response was obtained from the active VG samples when their surface temperatures were varied from 20^{o} to 65^{o}C. The vortex generators responded by increasing their angles of attack from 10^{o} to 38^{o} and as the designs were two-way trained, they regained their initial position and shape at a lower temperature. At their activated positions, maximum heat transfer improvements of up to 90 % and 80 % were achieved by the single and double wings respectively along the downstream direction. The flow pressure losses across the test section, when the wings were activated, increased between 7% and 63% of the losses at their de-activated positions, for the single and double VG respectively.

Key Words

Shape memory alloys, selective laser melting, active vortex generators, convective heat transfer, heat transfer enhancement.

Nomenclature

A	=	area, mm^2
B	=	heated plate width, mm
b	=	wing width, mm
c	=	wing chord length, mm
f	=	apparent friction factor
h	=	heat transfer coefficient, W/m^2K
h	=	VG height, mm
k	=	thermal conductivity, W/mK
L	=	length, mm
$\dot{m}$	=	mass flow rate, kg/s
Nu	=	Nusselt number, Nu = hH/k
Re	=	Reynolds number, $\rho VH/\mu$
s	=	VG spacing, mm
T	=	temperature, ^oC
V	=	velocity, m/s
x,y	=	streamwise coordinate, mm

Greek

α	=	wing angle of attack, ^{o}
Λ	=	wing aspect ratio, Λ=2b/c
μ	=	fluid dynamic viscosity, Pa.s

Subscript

avg	=	average
bm	=	bulk mean
f	=	fluid
H	=	channel height
o	=	de-activated position
s	=	surface

1. Introduction

The enhancement of heat transfer on heated surfaces is important in many engineering applications as it results in the use of less space and material, and allows for higher thermal loads. The key driver into this research has been the advancement in the miniaturization and design complexities of microelectronic devices in telecommunication and computing equipment. The increasing power dissipation densities of microelectronic devices are constantly monitored by the International Technology Roadmap (ITR) group which consists of globally renowned semiconductor manufacturers and research institutions. In the 2008 ITR report [1], the power densities of microelectronic devices (assembled packages) were predicted to increase by 50% in the year 2015. This implies an increase in surface temperatures and renewed thermal management challenges for semiconductor manufacturers. It is therefore important that research into heat transfer enhancement continues to receive the attention it needs to meet both the current and future demands.

Among the commonly studied heat transfer enhancement designs for heated surfaces is the so-called “Vortex Generator” (VG); a small surface protrusion that disturbs boundary layer flows. The earliest investigation into the use of VGs as a heat transfer enhancer was carried out by Edwards and Alker [2] in 1974. They compared surface mounted cubes and winglet designs and found that the winglets generated longitudinal vortices which had promising enhancement capabilities.

As a longitudinal VG, the delta wing generates vortices which mix the cooler free stream fluid with the warmer air just above the heated surface, as shown in Fig. 1. Persisting vortices in the flow direction extends the cooling effect on the heated plate several wing chord lengths downstream of the VG. Among the important factors which influences the enhancement capability of a delta wing VG is its geometrical features ie. angle of attack and aspect ratio. Fig. 2 illustrates several surface protrusion designs, including the delta wing, with definitions of their geometrical features.

Early investigations into the enhancement effects of increasing the angle of attack, α, were carried out by Fiebig et al. [4] for delta wings placed on a fin surface, in a heated rectangular channel. The test section was supplied with developing laminar air flow for Reynolds numbers, Re_H, based on the channel height, between 1360 and 2270. By increasing α from 10^o to 50^o, an average heat transfer enhancement of 60% was obtained on the surface downstream of the delta wings compared to a plane surface. The negative effect of the delta wing VG is, however, the increased frictional loss and the obstruction it causes to the flow over the heated surface which contribute to pressure losses. Fiebig et al. found that by increasing the angle of attack of the delta wing, the flow pressure loss across their test section increased by as much as 15% compared to an unobstructed surface. Another important finding reported from their experiment was that the channel walls of their test section had prevented early vortex break down. This is a common vortex generation problem in unbounded test sections where VGs with high angles of attack are used. Their research provided a qualitative description of the vortex shape, intensity and location in the downstream regions of the VG which gave further insight into the use of the delta wing as a heat transfer enhancement device. In a subsequent investigation, Fiebig et al. [5] varied the aspect ratio, Λ, of the delta wing and compared their heat transfer enhancements for a range of α at a fixed laminar flow Reynolds number. As a result of varying Λ from 0.8 to 1.5, increases in heat transfer enhancement by as much as 10% was obtained when α of between 10^o and 50^o were compared. Apart from increasing α and Λ, and preventing early vortex breakdown, channel walls have been found to provide positive effects on heat transfer enhancements for VGs. Fiebig et al. [4,5] and Biswas et al. [6] reported that the channel walls, through increasing pressure gradients in the downstream direction, keep the longitudinal vortices stable and effective in their respective paths for a longer downstream distance, and hence provide higher overall heat transfer improvements.

Jacobi and Shah [7], in their review of experiments and numerical studies on heat transfer enhancement techniques carried out by various researchers, compared surface protrusion and extended surface designs such as cubes, plate-fins, round and flat tube rows, delta and rectangular wing and winglet vortex generators. Amongst the surface protrusion devices, the delta wing and winglet geometries were the most frequently studied (see Fig. 2). In rectangular channels, the highest overall heat transfer enhancement, as high as 60% compared to a plain channel, was obtained by Fiebig et al. [5] and Tiggelbeck et al. [8] for a single delta wing supplied with air flow in a 1300 to 2300 Reynolds number range. The heat transfer improvement from the single delta wing was accompanied by a 45% increase in flow pressure losses. When pairs of delta winglets were arranged in in-line and staggered arrangements, relatively higher heat transfer improvements were obtained for similar Reynolds numbers. The winglet arrangements, however, contributed to significantly higher flow pressure losses, up to 145%, compared to unobstructed channel surfaces. From their review of previous investigations, Jacobi and Shah recommended the use of high angles of attack, between 40^o to 50^o and aspect ratios of between 1.8 and 2 for single delta wings, particularly for use in channel flows. The increases in flow pressure losses which result from the high angles of attack of the single delta wing were reasonably low for the flow conditions explored. Further considerations, however, would be required for different flow conditions and for the use of multiple vortex generators, to prevent excessive flow pressure losses.

Gentry [9], together with Jacobi [10,11], revisited earlier research carried out on delta wing VGs and reported, in more depth, the effects of the vortices on heat transfer enhancement and flow pressure losses. Unlike other investigations, the effects of the VG location close to the leading edge of a test section were explored. They measured vortex strength for the various angles of attack and for different wing aspect ratios. This was done by two methods: a) by direct measurement using a vane-type vortex meter and b) using a potential-flow model and flow visualization technique. Their work supported what earlier results suggested, and managed to quantify the vortex strength at various positions downstream of the VG. They had identified from their results an α of 45^{o} and Λ of 1.2 as suitable parameters for heat transfer enhancement from a delta wing VG. Close to the test section leading edge, it was found that the vortex strength increased, an occurrence which is believed to be due to the VG wing tips staying above the surface's developing hydrodynamic boundary layer thickness.

In turbulent flow conditions, interaction between vortices and the hydrodynamic boundary layer is expected to be significantly different from laminar flow conditions. Eibeck and Eaton [12] evaluated the mean streamwise vortices developed from a single vortex generator, on a flat surface. The enhancement of heat transfer within the turbulent boundary layer was found to be a result of the vortices imposing local modifications in the heat transfer coefficient through the distortion of the mean flow, and not due to turbulent transport.

Investigations into the application of more than one VG have only been reported, in open literature, for the winglet type designs. The main concern over the installation of multiple VGs in channels or flat surfaces, as highlighted by Pauley and Eaton [13], was the optimum VG spacing. In their investigations, experiments were carried out on a pair of delta winglets in turbulent flow conditions, and from which, the mean heat transfer enhancements on the downstream areas were evaluated. The similarities observed in the experimental results with regard to the vortex swirl direction and their affects on heat transfer enhancement, in both turbulent and laminar flow, suggests the independence of the vortex induced cooling mechanisms in the different flow conditions. The smallest recommended VG spacing, s, between the tips of the delta winglet pair is equal to the height of the winglet, h; a smaller spacing results in the inability of the winglets to generate vortices. For $h < s < 2h$, the vortex strength was found to be independent of s, while for $s > 2h$, lower vortex strengths at the same streamwise location was observed.

Although proven to be good heat transfer enhancers, the main issue related to the use of wing and winglet type VGs have been the flow pressure losses, especially when set to operate at high angles of attack. A solution suggested by Jacobi and Shah [7] was to use active vortex generators. The active designs and methods which were proposed included electrohydrodynamics, acoustics and wall jets. These designs however require the use of external sources which are impractical with regard to cost, operation and maintenance issues.

One method of introducing active heat transfer enhancement without relying on external sources is by fabricating the enhancement devices from shape memory alloys. An equiatomic alloy of TiNi, commonly referred to as Nitinol, is known to have stable shape memory effects and has been commercially used as pipe couplers, fittings, valve actuators, electrical connectors and telecommunication components [14]. The two modes of responses which characterise a shape memory alloy are superelasticity and thermal shape memory effect. The thermal shape memory effect refers to the ability of a shape memory alloy to undergo a shape transformation in response to a temperature change, and is a characteristic which has not been exhaustively explored for heat transfer enhancement applications. Champagne and Bergles [15] reported on the use of Nitinol helical springs on the internal walls of pipes, aligned to the flow direction, to produce a variable surface roughness effect for heat transfer enhancement. The springs, between their activated and de-activated positions, were able to achieve heat transfer enhancements of approximately 64%. The accompanying increase in flow pressure losses was approximately 25%. The novel in-tube variable roughness design, however, encountered the following problems: (1) only one-way thermal shape memory effect was obtained by the active springs, (2) there were difficulties in mounting the active springs to the internal pipe walls while giving access for a manual reset of their shapes after being activated, and (3) the spacer-support structure along the internal pipe walls which held the springs in place was contributing towards significant fixed flow pressure losses. These issues were a major set-back for further progress into their research and, to this date, to the present authors' knowledge, no reports on further developments of similar designs or applications are available in open literature.

In a recent investigation the present authors [16,17] explored the development of active heat transfer devices manufactured from shape memory alloys for the cooling of an exposed heated surface. The proof-of-concept study focused on active delta wing VG designs manufactured in an advanced rapid prototyping process known as Selective Laser Melting

(SLM); a process which involves the melting of metallic powders with a continuous wave Ytterbium fibre laser in layer-additive steps. Readers are asked to refer to references [16,17] for a more comprehensive explanation on the SLM process. Their designs were successfully manufactured using pre-alloyed Nitinol powder, and were two-way trained to respond to a high and low temperature of 65^{o}C and 20^{o}C respectively. As the focus of the work was to explore the concept of active vortex generators from shape memory alloys, not much attention was given to the acquisition of heat transfer enhancement and pressure loss data.

In the present investigation an experiment was carried out to determine the heat transfer enhancement and flow pressure losses due to the presence of active VGs, manufactured from shape memory alloys, on a heated rectangular channel surface. Delta wings were chosen as the active VG design for their geometrical simplicity and proven heat transfer enhancement capabilities. The potential application of the active delta wing(s) would be as heat transfer enhancers in microelectronics systems. Another important aspect of the active VGs explored in this work is that they were made in an SLM process which offers various advantages compared to commercially available shape memory alloy designs. To evaluate the heat transfer enhancement effects, Infrared Thermography was used to acquire surface temperature data downstream of the VG. Low air flow velocities were used in the experiment to closely match the flow conditions available in actual electronics cooling applications.

2. Experimental Study

The experimental work presented in the following sections were carried out to train, test the functionality of the respective VG designs and to explore the heat transfer and pressure loss reduction capabilities of the active devices.

2.1 Shape Memory Alloy

Shape memory alloys (SMAs) are commercially available in the form of thin sheets, bars, slabs and wires of various sizes. Presently, these available forms of SMAs need further post processing to obtain the required design features and shape memory alloy characteristics before they can be utilized. One way of simplifying the various stages in the design, manufacturing and the application of an SMA component is through the use of the SLM process. The SMA components from this process are built to recognize their high temperature shape and therefore eliminate the requirement for further shape-setting heat treatment whereas the sheet form, for example, requires prior heat treatment to set its high temperature shape. The SLM process is also capable of manufacturing designs with complex geometric features, possibly making them more adaptable for microelectronic cooling applications.

The successful use of SLM in fabricating Nitinol designs such as actuators, flow control devices and vortex generators were reported by the present authors in [16,17] and by Clare et al. [18]. Their designs were tested and found to have two-way shape memory effect characteristics.

For the current work, pre-alloyed Nitinol (Ti-50at% Ni) powder having an average particle size of 75μm was used to manufacture the delta wing VGs in an MCP-Realizer SLM-100 machine [19]. The VGs were manufactured to the following geometric specifications:

Angle of attack, α	=	45^{o}
Aspect ratio, Λ	=	2
Thickness, t	=	100 μm.

The fabricated samples were later two-way trained, using the martensite-deformation technique recommended by Lahoz et al. [20], between a high and low temperature set point as illustrated in Fig. 3. The angles of attack of these samples were measured at their activated and deactivated positions after 20 training cycles.

2.2 Delta Wing Vortex Generators

The active VG samples used in the present work were arranged as a single VG and a pair of VGs, each adhered to the surface of a 10 mm thick aluminium plate. The VG devices were located as close as possible to the leading edge of the test section (x/L=0.1) as shown in Fig. 4. This is to take advantage of the longitudinal vortex effects which were previously reported by Fiebig et al. to persist for at least 7.5 chord lengths downstream of the VG [3]. Their paper also identified the lateral distribution of heat transfer enhancement behind the VG which was taken into consideration in determining the pitch distance for the VG pair in the present work. The heat transfer enhancement effects, as a result of the samples being activated and deactivated at their respective temperature set points, are reported along the streamwise (x/L) and spanwise (y/B) directions of the heated surface.

2.3 Heat Transfer Enhancement and Pressure Loss

The experimental work to investigate the heat transfer enhancement and flow pressure losses from the active delta wing VGs was carried out in a small air flow rig consisting of a test section, inlet and outlet ducts, sensors and instrumentation for data acquisition. A schematic of the experimental set up is shown in Fig. 5.

A uniform temperature condition was achieved at the base of the test section by using a 16mm thick copper block, heated by two, 6mm diameter cartridge heaters controlled by a variable AC power supply and control unit. The side walls of the test section were heavily insulated with Armacell insulation to ensure minimal heat loss; the radiation and conduction losses from the test section without the insulation were estimated at 4% of the total heat supplied to the test section. The inlet, test section and outlet duct have a uniform rectangular cross sectional area of 10mm (high) x 50mm (wide) and a total length of 2800mm. To ensure that the flow entering the test section is fully developed, air at ambient conditions is forced through the air supply section which consisted of flow straighteners and an inlet duct length of 60 hydraulic diameters. Fully developed flow in the test section is important as it would demonstrate the true effects of the generated vortices on boundary layer thinning. The Reynolds number, Re_H for the experiment was determined based on the channel height, H of the duct and had a range of between 1573 and 3712. The air inlet and outlet temperatures were measured by two sets of four T-type thermocouples, each set placed 60mm before and after the test section, while the surface temperature of the test section was obtained from infrared thermography. A FLIR-SC500 infrared camera was used to acquire surface temperature data at streamwise and spanwise distances x/L and y/B, behind the VG. The camera had an emissivity spectrum of 7.5 - 13 μm and a resolution of 320 x 240 pixels at a frame rate of 50 Hz. An illustration of the surface temperature measurement points with respect to the VG location and leading edge of the test section are shown in Fig. 6. Infrared access into the test section was obtained through a 50 mm diameter infrared sight glass with a transmissivity of 0.96. The heated surface of the test section was painted with matt-black paint which was measured, by an in-situ technique, to give an emissivity of 0.92. In-situ calibration of the captured infrared image was carried out with a surface mounted thermocouple over a 40 – 150 ^{o}C range.

The local heat transfer enhancements were determined from the ratio of the local Nusselt numbers at the sample's activated and de-activated positions, Nu/Nu$_o$. The calculations for the local Nusselt numbers were based on the following equation:

$$Nu = \frac{\dot{m} C_p (T_{in} - T_{out})}{A_s (T_x - T_{bm}) k_f} H \qquad (1)$$

The average heat transfer enhancement, $Nu_{avg}/Nu_{avg,o}$, was determined for the heated surface area downstream of the VG sample. The average enhancement ratio considers the streamwise and spanwise effects of the vortices on a fixed surface area, and provides a general indication of VG performance.

A non-dimensional form of the flow pressure loss across the test section, also known as the apparent friction factor, *f*, is determined from the following equation,

$$f = \frac{\Delta P \cdot H}{L \frac{1}{2} \rho V_{avg}^{2}} \qquad (2)$$

and used in the ratio, f/f_o, to obtain the increase in flow pressure losses between the VG's activated and de-activated positions. A differential pressure transducer (Omega PX 653-10D5V), based on tapping points located 50 mm before and after the test section, gave measurements of static pressure drop, ΔP across the test section. For test section velocity and flowrate measurements, a single probe hot wire anemometer system (Dantec Dynamics) and a thermal mass flow meter (Endress and Hauser AT70F) were used respectively. The hot wire anemometer readings were taken at different locations across the outlet duct cross sectional area and an average value was calculated to represent the flow through the test section.

The experimental uncertainties for the variables in equations (1) and (2) were calculated using the Kline and McClintock's 2nd Power Law [21]. The worst case uncertainties for the air temperature, mass flow rate and flow pressure loss measurements were +/- 2%, +/-6% and +/-12% of their respective average values (at the 95% confidence level).

3. Results and Discussion

Prior to conducting the heat transfer experiment, the delta wings were tested for their functionality as active VGs. They were found to respond to a high temperature set point of 65 ^{o}C by deforming into a complete featured vortex generator at $\alpha_{active} = 38^{o}$ and returning to a low profile ($\alpha_{deactivated} \approx 10^{o}$) at a temperature set point of 20 ^{o}C. The actual angles of attack measured during the functionality test differed from their design values as there were losses from the metallurgical defects in the material during the thermal training cycles. The stabilised working angles of attack for the SLM manufactured VGs in the present study were, however, in close agreement with earlier results reported in [16,17].

The heat transfer enhancement effects and flow pressure losses were determined for a single and a pair of active VGs. The flow pressure loss ratios in this experiment are of course in relation to the specific duct geometry to illustrate the pressure loss advantage of active VGs; a different height duct, for example would yield different values.

3.1 Heat Transfer Enhancements and Pressure Losses from Active Vortex Generators

The streamwise and spanwise enhancement effects reflect the local heat transfer enhancement distribution on the test section surface downstream of the VG. The experimental work carried out over a Re_H range of 1573 to 3712 found that the highest enhancement effects occur at its highest Reynolds number of 3712. The data related to Re_H=3712 was later chosen for presentation in this paper to demonstrate the effects of active VGs in conditions that might be found in typical microelectronic cooling applications.

The heat transfer enhancements from the small angles of attack at the VGs' deactivated positions were found to average at approximately 12% for the single VG and 15% for the VG pair, compared to a flat test surface. The accompanying increase in flow pressure losses at the de-activated angles, for all the VG arrangements, were found to be less than 5% compared to a flat test surface.

The Nu/Nu_o graph shown in Fig. 7 represents the streamwise enhancement effects from a single VG at a Re_H of 3712. It is evident from this graph that there is an increase in heat transfer along the length of the heated surface as a result of the VGs being activated. A maximum heat transfer enhancement of 28% between the activated and deactivated positions was found approximately one chord-length behind the VG (x/L=0.2), along the centreline of the heated surface (y/B=0.5). The higher heat transfer enhancement at the one chord-length distance is due to the intense mixing of the free stream and boundary layer fluid, as described by Gentry et al. [10] in their previous work on the measurement of vortex strength downstream of fixed delta wing VGs. A similar enhancement pattern for laminar flows over fixed delta wings was observed in experiments carried out by Fiebig et al. [4,22] and numerical predictions by Biswas et al. [6,23]. Further downstream, along the centreline of the heated surface (y/B=0.5), between streamwise locations, x/L of 0.24 and 0.42, the enhancement effect is seen to decrease sharply from its maximum value and stabilise at an average enhancement of about 18%. Similar trends were observed for other measurement points close to this centreline, where a narrow cooling band was formed along the streamwise direction of the test section. Another observation to be made from the streamwise data in Fig. 7 is how the outer regions (rows 1-2 and 22-23) have relatively lower enhancement effects but gradually show improvements and match-up to the mid-section enhancement data further downstream of the VG. The spanwise enhancement trend in the present study is consistent with previous studies reported by Fiebig et al. [5] and Gentry et al. [10] in which the longitudinal vortices from fixed delta wings were found to propagate in a narrow path before spreading outwards after two to three chord-lengths downstream of the VG, explaining the lower enhancements for the outer regions on both sides of the VG trailing edge (x/L=0.10).

A further illustration on the variation of enhancement effects in the spanwise direction of the test section is shown in Fig. 8 for the single VG. Similarities in the spanwise variation obtained here, with the work of Fiebig et al. [5] were observed; in both cases, the dominant tip vortices provided higher heat transfer in a narrow region close to the centreline of the VG. Further downstream, a wider spread of enhancement effects were represented by a flatter distribution from x/L = 0.24 to 0.34 compared to x/L=0.2. The higher aspect ratio of the VG used in the present study has resulted in the enhancement effects covering a much wider area (approximately three times the VG width) as compared to the smaller aspect ratios used in previous investigations [4,5,9,22].

The streamwise enhancement effects from a pair of active VGs at Re_H = 3712 is shown in Fig. 9. Similar to the active single VG, the enhancement trend along the streamwise direction is seen to start off at a significantly high value and decay further downstream. The peak heat transfer enhancement between the active and deactivated VG positions was found to be 170%, compared with just 28% for the single active VG at the same streamwise location. There is a sharp drop in enhancement effects between x/L= 0.22 and 0.24 after which it steadily decreases until an average of 115% is reached at approximately four chord lengths downstream of the VGs.

Observing the enhancement variation in the spanwise direction of the VG pair, as shown in Fig. 10, the maximum value is found close to the centrelines of each VG at x/L=0.20, and they tend to decrease toward the middle of the test section. The space between the VGs, chosen based on the recommendation by Pauley and Eaton [13], did not significantly reduce enhancements as the effects of vortices were still present in this region. The interaction between neighbouring vortex paths, however, was seen further downstream, between x/L=0.24 and 0.34, and resulted in a more uniform enhancement effect compared to the single VG arrangement. The effect of tail-end vortices from the VG-pair is seen downstream of x/L=0.52. Here, the already weak vortices leave an area of lower enhancement (albeit approximately 120%) in the middle of the test section whilst it disperses to the sides and contributes to the heat transfer enhancements there.

A comparison of the average heat transfer enhancement at each streamwise location for the VG pair and the single-VG arrangement is shown in Fig. 11. Here, the average heat transfer enhancements, Nu_{avg} / $Nu_{avg,o}$ at Re_H = 3712, for the single VG and VG pair arrangements, were found to be 17% and 133% respectively. Apart from highlighting the difference in heat transfer enhancement capabilities, a much more uniform streamwise variation, throughout the test section length, is observed for the VG arrangements.

The advantage of having active VGs is their ability to maintain a low flow pressure-loss position when they are deactivated, taking advantage of the high angles of attack only when it is necessary to enhance cooling at high temperatures. To demonstrate the effects of the active and deactivated VG positions on a "geometry dependent" pressure loss in the test section, the apparent friction ratio, f/f_o was calculated for the single VG and VG pair. At the Re_H used to evaluate heat transfer performance, compared to their respective de-activated positions, the single VG in its active position contributed towards a 39% pressure loss while the flow obstructions from the active VG pairs contributed to 63% pressure loss. The pressure loss results support the use of active features in VGs as they imply significant savings in the required pumping power when VG arrays are used to achieve higher heat transfer enhancements.

4. Conclusion

The investigation into the use of active delta wing vortex generators made from shape memory alloy material was successfully carried out. The delta wings were built to their active positions in the SLM process, reducing further heat treatment as often required by commercially available shape memory alloy material. A two-way shape memory effect was obtained between a high and low temperature set point after 20 training cycles had been carried out on the samples. This gave the samples their active characteristics i.e. intruding into the flow to generate vortices that promote air flow mixing resulting in heat transfer enhancement.

As active vortex generators at their activated positions, maximum heat transfer improvements of up to 90 % and 80 % were achieved by the single and double wings respectively along the downstream direction. The corresponding flow pressure losses across the test section, when the wings were activated, increased between 7% and 63% of the losses at their de-activated positions, for the single and double VG respectively. Although the pressure loss increase was high, it occurred only when the VGs were active and was outweighed by the VG's contribution to heat transfer.

Both the heat transfer and pressure loss results from this experiment have demonstrated the ability of active vortex generators as heat transfer enhancers. Although the active vortex generators developed in this research were scaled and tested for microelectronics applications, they still have great potential for use in a variety of different applications such as in the automotive and aerospace industries.

5. Acknowledgement

The authors wish to thank Dr. Tim Jones, Mr Lawrence Bailey and Mr. Derek Neary for their valuable technical support and advice on the experimental set up.

6. References

[1] International Technology Roadmap for Semiconductors, 2008 Ed. (Assembly and Packaging-Table AP2a, 2b), www.itrs.net/reports accessed: 15/01/10

[2] F. J. Edwards and C.J.R. Alker, The improvement of forced convection surface heat transfer using surface protrusions in the form of (a) cubes and (b) vortex generators, Proceedings of the Fifth International Heat Transfer Conference, JSME, Tokyo, Japan, 1974, pp. 244-248.

[3] Gursul, I., Reveiw of unsteady flow over slender delta wings, Journal of Aircraft, 42(2) 2005, pp. 299-319.

[4] M. Fiebig, Wing type vortex generators for heat transfer enhancements, Proceedings of the Eighth International Heat Transfer Conference, 1986, pp. 2909-2913.

[5] M. Fiebig, Embedded vortices in internal flow: heat transfer and pressure loss enhancement, International Journal of Heat and Fluid Flow, 16 (5) (1995) 376-388.

[6] G. Biswas and H. Chattopadhyay, Heat transfer in a channel with built-in wing type vortex generators, International Journal of Heat and Mass Transfer 35 (4) (1992) 803-814.

[7] A.M.Jacobi and R.K. Shah, Heat transfer surface enhancement through the use of longitudinal vortices: a review of recent progress, Experimental Thermal and Fluid Sciences 11 (1995) 295 – 309.

[8] S. Tiggelbeck, N.K. Mitra, M. Fiebig, Experimental investigations of heat transfer enhancement and flow losses in a channel with double rows of longitudinal vortex generators, International Journal of Heat and Mass Transfer 36 (9) (1993) 2327-2337.

[9] M.C. Gentry, Heat transfer enhancement using tip and junction vortices, PhD thesis, University of Illinois, Urbana-Champaign, IL, 1998.

[10] M.C. Gentry and A.M. Jacobi, Heat transfer enhancement by delta wing vortex generators on a flat plate: vortex interactions with the boundary layer, Experimental Thermal and Fluid Sciences 14 (3) (1997) 231-242.

[11] M.C. Gentry and A.M. Jacobi, Heat transfer enhancement by delta wing generated tip vortices in flat plate and developing channel flows, Journal of Heat Transfer 124 (6) (2002) 1158-1168.

[12] P.A. Eibeck and J.K. Eaton, Heat transfer effects of a longitudinal vortex embedded in a turbulent boundary layer, Journal of Heat Transfer 109 (1) (1987) 16-24.

[13] W.R. Pauley and J.K. Eaton, The effect of embedded longitudinal vortex arrays on turbulent boundary layer heat transfer, Journal of Heat Transfer 116 (4) (1994) 871-879.

[14] Otsuka, K. And Wayman, C.M., Shape Memory Materials, Cambridge, Cambridge University Press, 2nd Ed. (1998)

[15] P.R. Champagne and A.E. Bergles, Development and testing of a novel, variable-roughness technique to enhance, on demand, heat transfer in a single-phase heat exchanger, Enhanced Heat Transfer 8 (2001) 341-352.

[16] M.S. Aris, I. Owen and C.J. Sutcliffe, The application of shape memory alloy as vortex generators and flow control devices for enhanced convective heat transfer, Proceedings of the Fifth Joint ASME/JSME Fluids Engineering Conference, ASME, San Diego, Ca, 2007, FEDSM2007-37080.

[17] M.S. Aris, I. Owen and C.J. Sutcliffe, The application of shape memory alloy as longitudinal vortex generators for enhanced convective heat transfer, Proceedings of the Tenth UK Heat Transfer Conference, Edinburgh, Scotland, 2007.

[18] A.T. Clare, P.R. Chalker, S. Davies, C.J. Sutcliffe and S. Tsopanos, Selective laser melting of high aspect ratio 3D nickel titanium structures two way trained for MEMS applications, International Journal of Mechanics and Materials in Design 4(2) (1998) 181-187.

[19] MTT technologies group, http://www.mtt-group.com/selective-laser-melting.html, Retrieved 21st July, 2009

[20] R. Lahoz, L. Grasia, J.A. Puertolas, Training of the two-way shape memory effect by bending in NiTi alloys, Journal of Engineering Materials and Technology 124 (2002) 397-401.

[21] R.S. Figliola and D.E. Beasley, Theory and Design for Mechanical Measurements, John Wiley and Sons, New York, 1991, pp148-150.

[22] M. Fiebig, P. Kallweit, N.K. Mitra and S. Tiggelbeck, Heat transfer enhancement and drag by longitudinal vortex generators in channel flow, Experimental Thermal and Fluid Sciences 4 (1) (1991) 103-114.

[23] G. Biswas, K. Torii, D. Fujii and K. Nishino, Numerical and experimental determination of flow structure and heat transfer effects of longitudinal vortices in a

channel flow, International Journal of Heat and Mass Transfer 39 (16) 1996 3441-3451.

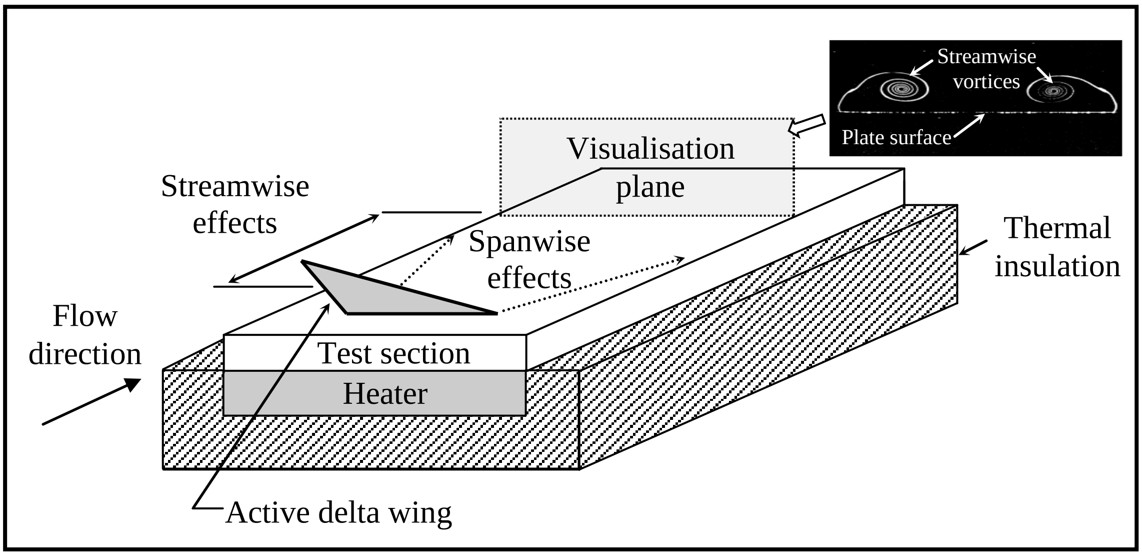

Figure 1: Vortex formation downstream of a delta wing (adapted from Gursul [3])

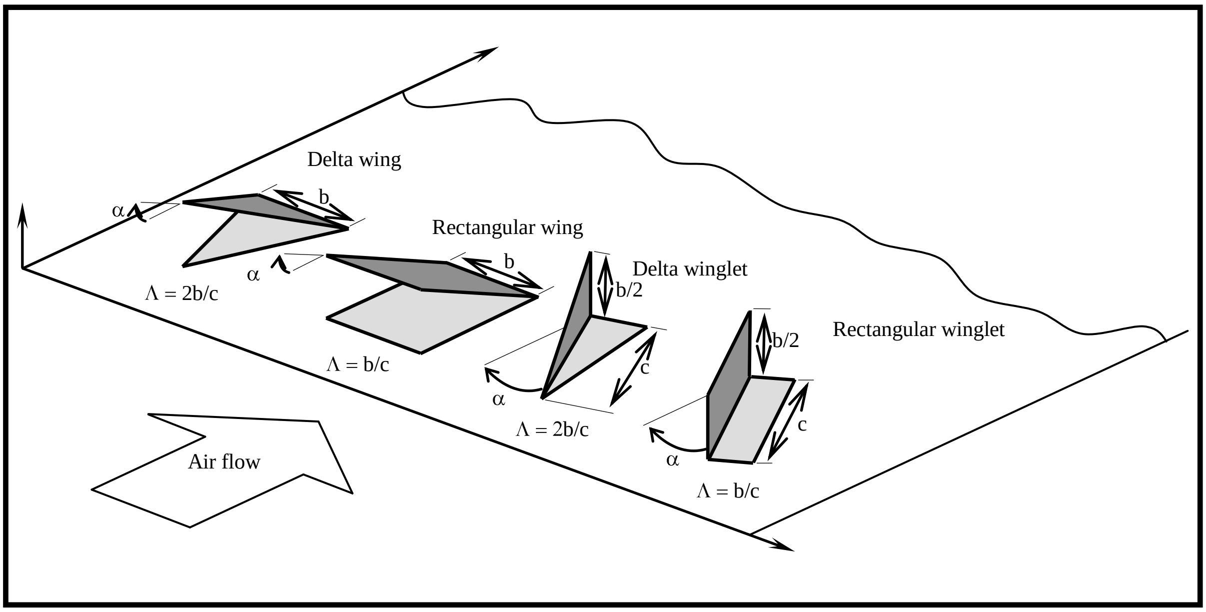

Figure 2: Common surface protrusions and their associated geometrical definitions

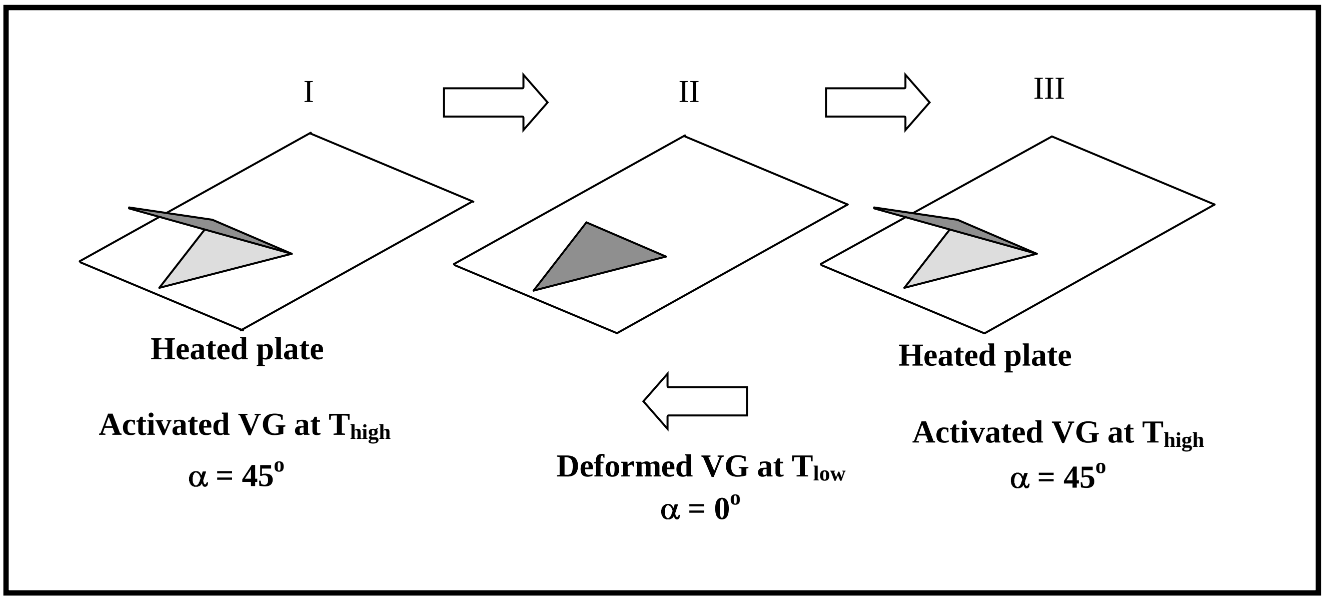

Figure 3: **Thermal training cycle for two-way shape memory effect between high and low temperature set points**

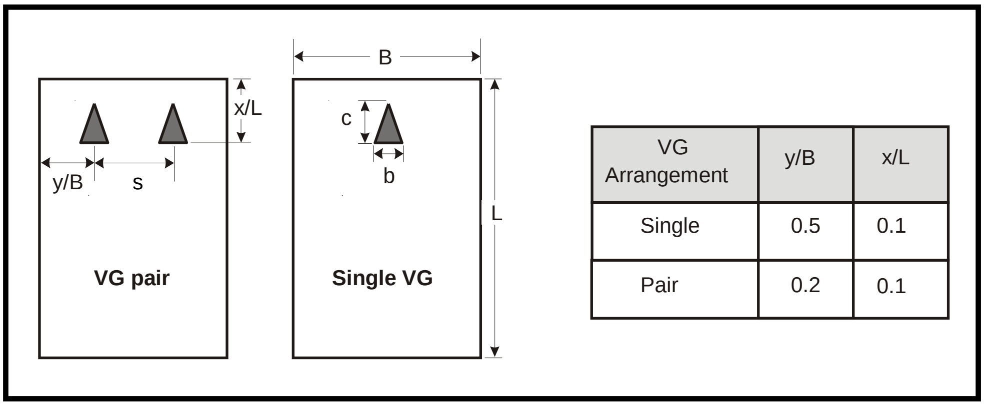

Figure 4: **VG locations on the test surface given in terms of their streamwise and spanwise distances, x/L and y/B**

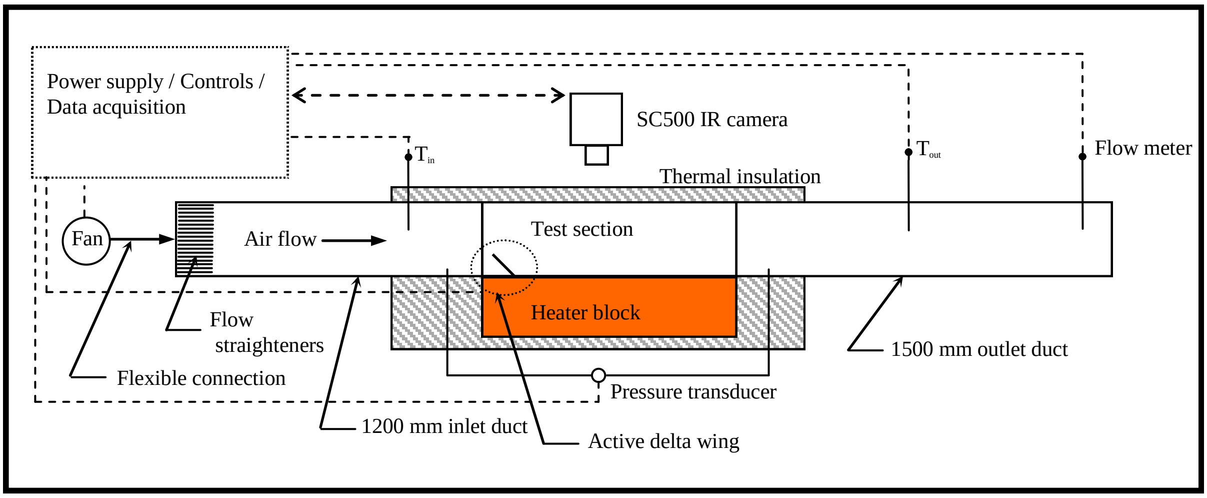

Figure 5: Heat transfer enhancement air-flow test rig

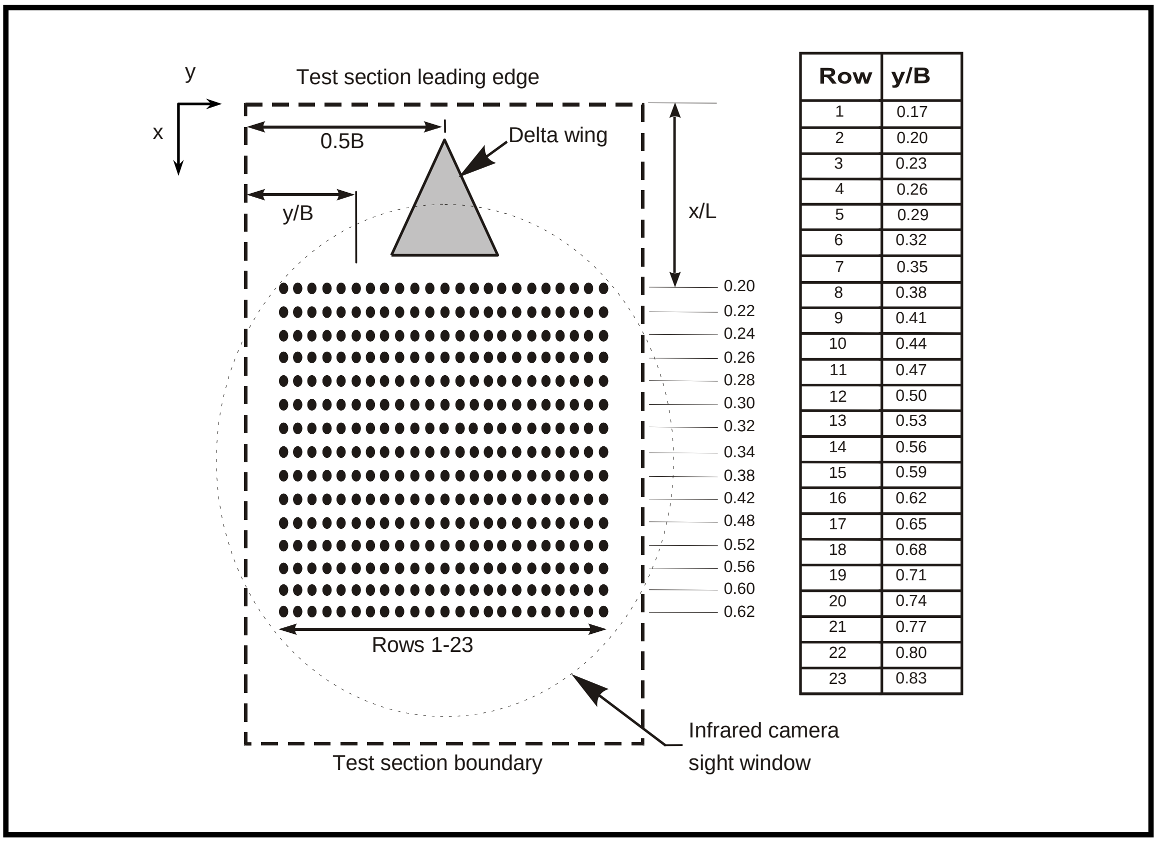

Row	y/B
1	0.17
2	0.20
3	0.23
4	0.26
5	0.29
6	0.32
7	0.35
8	0.38
9	0.41
10	0.44
11	0.47
12	0.50
13	0.53
14	0.56
15	0.59
16	0.62
17	0.65
18	0.68
19	0.71
20	0.74
21	0.77
22	0.80
23	0.83

Figure 6: Temperature measurements on the test surface

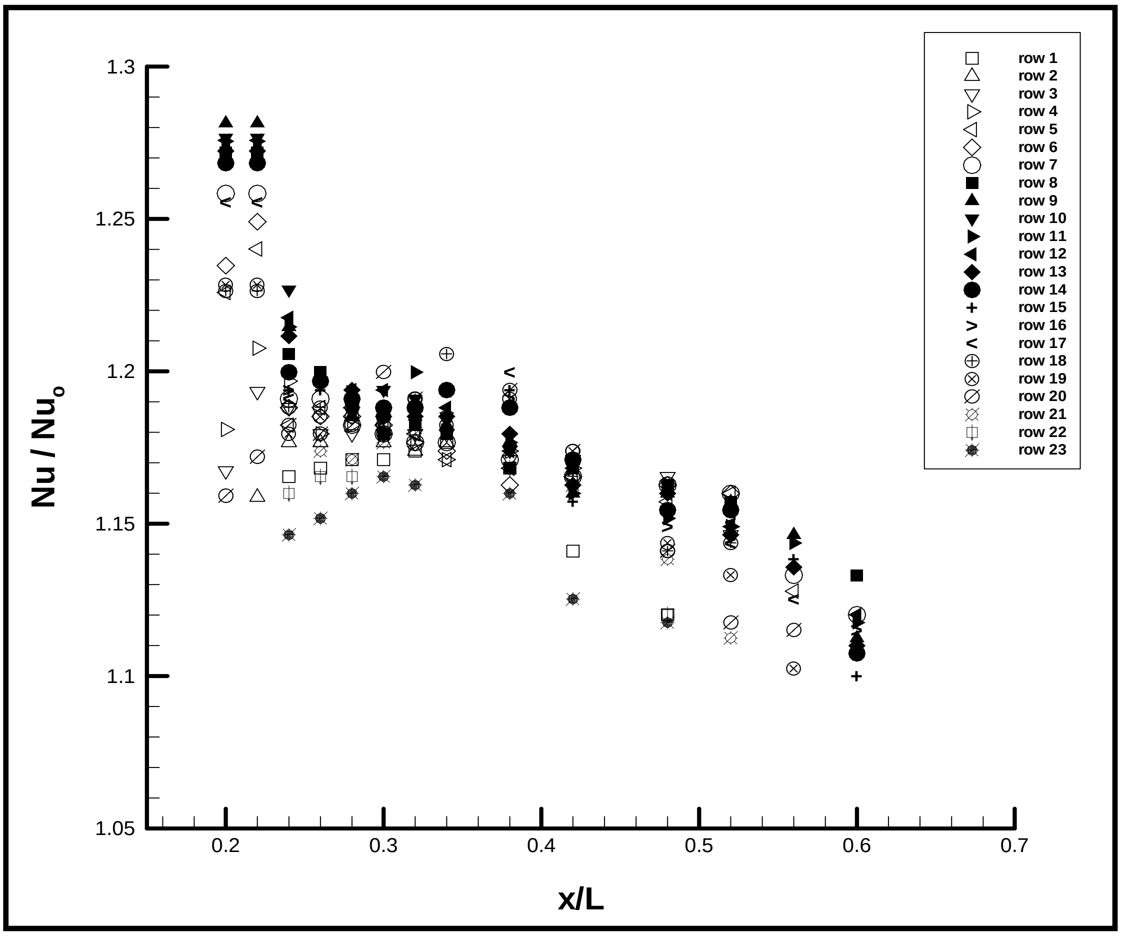

Figure 7: Streamwise heat transfer enhancement for a single VG at Re_H=3712

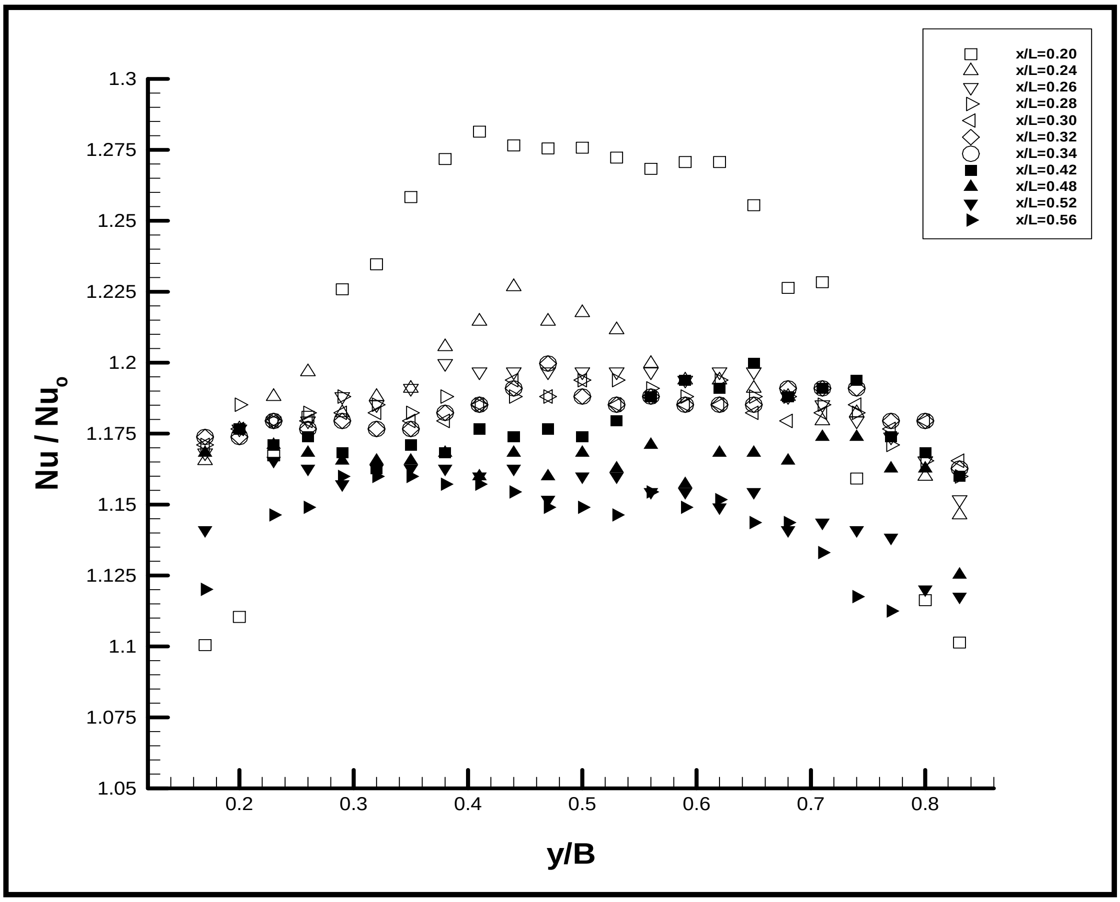

Figure 8: Streamwise heat transfer enhancement for a single VG at Re_H=3712

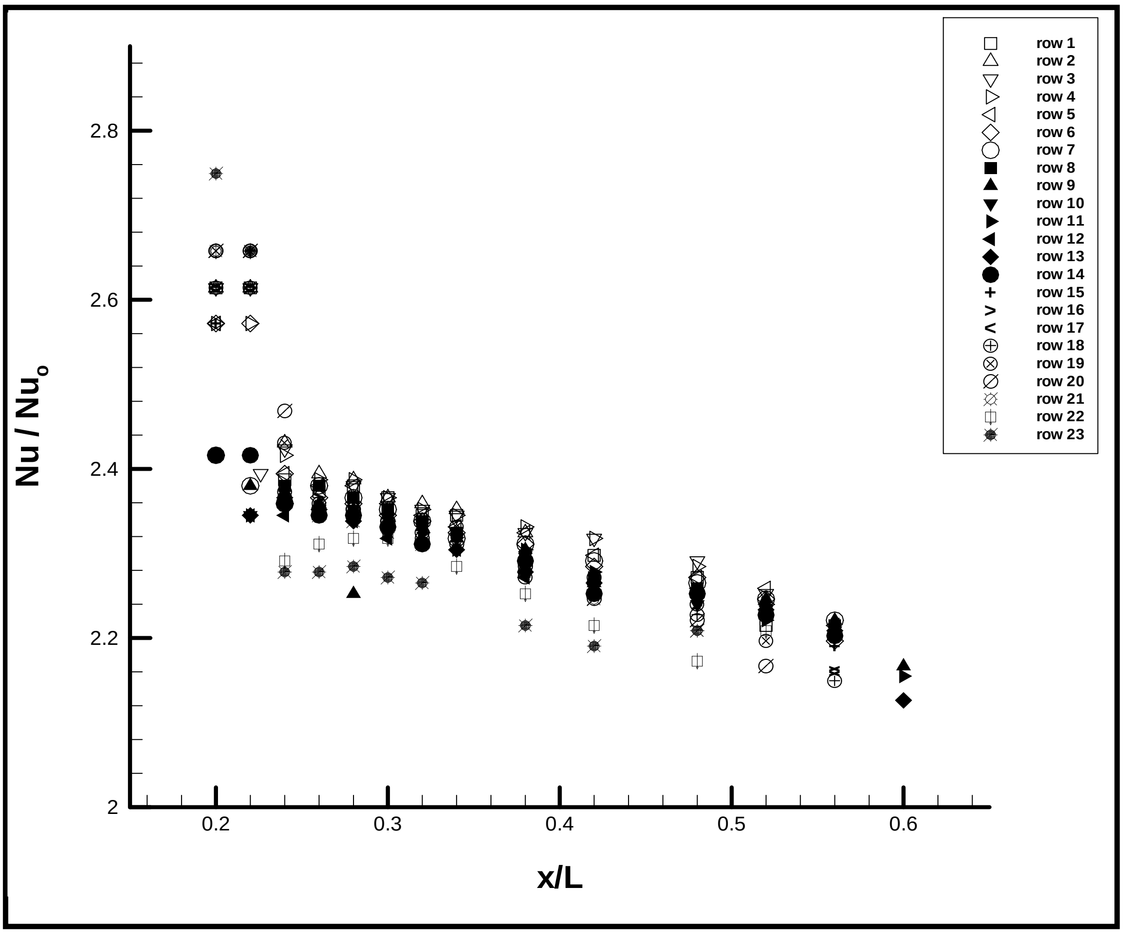

Figure 9: Spanwise heat transfer enhancement for a single VG at Re_H=3712

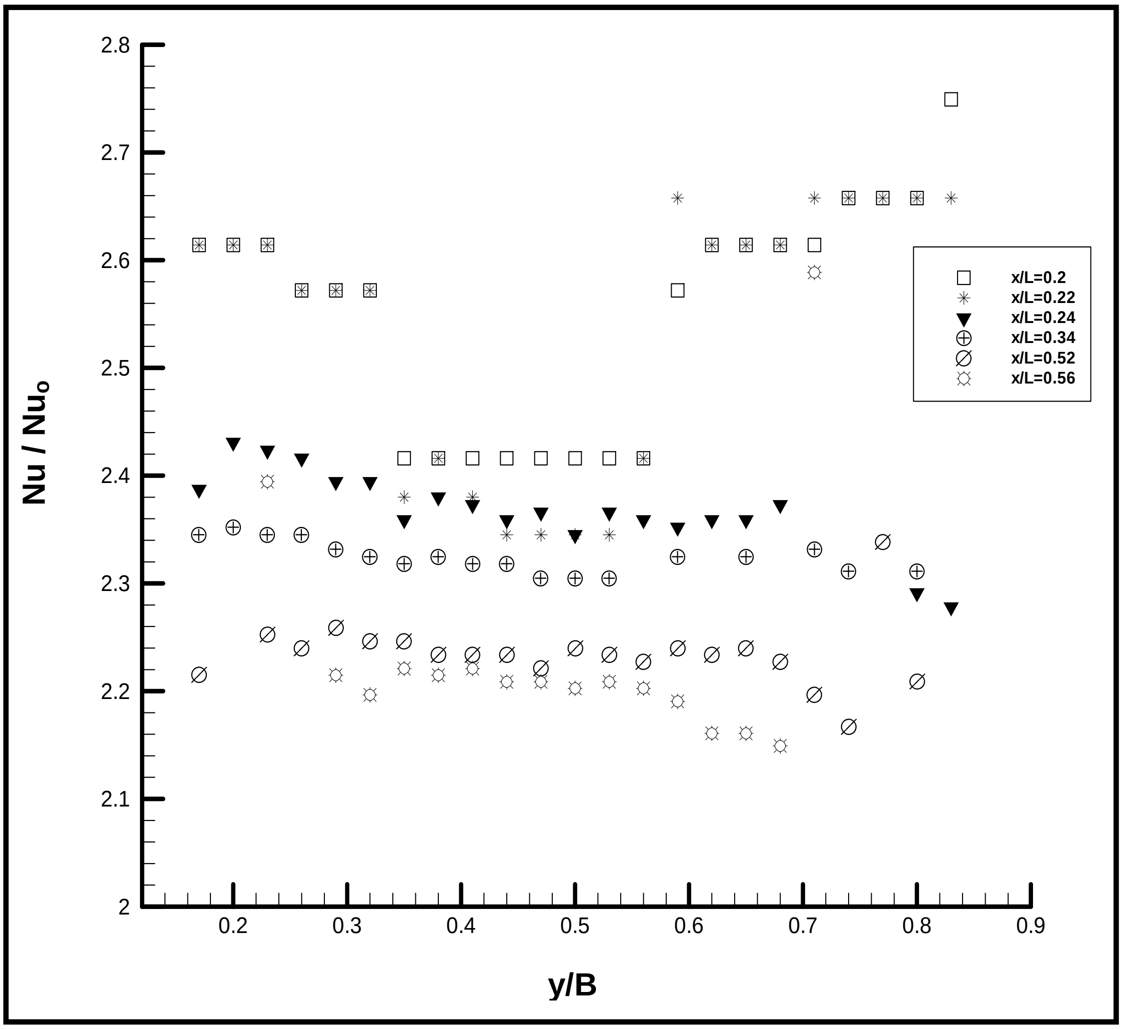

Figure 10: Spanwise heat transfer enhancement for a double VG at Re_H=3712

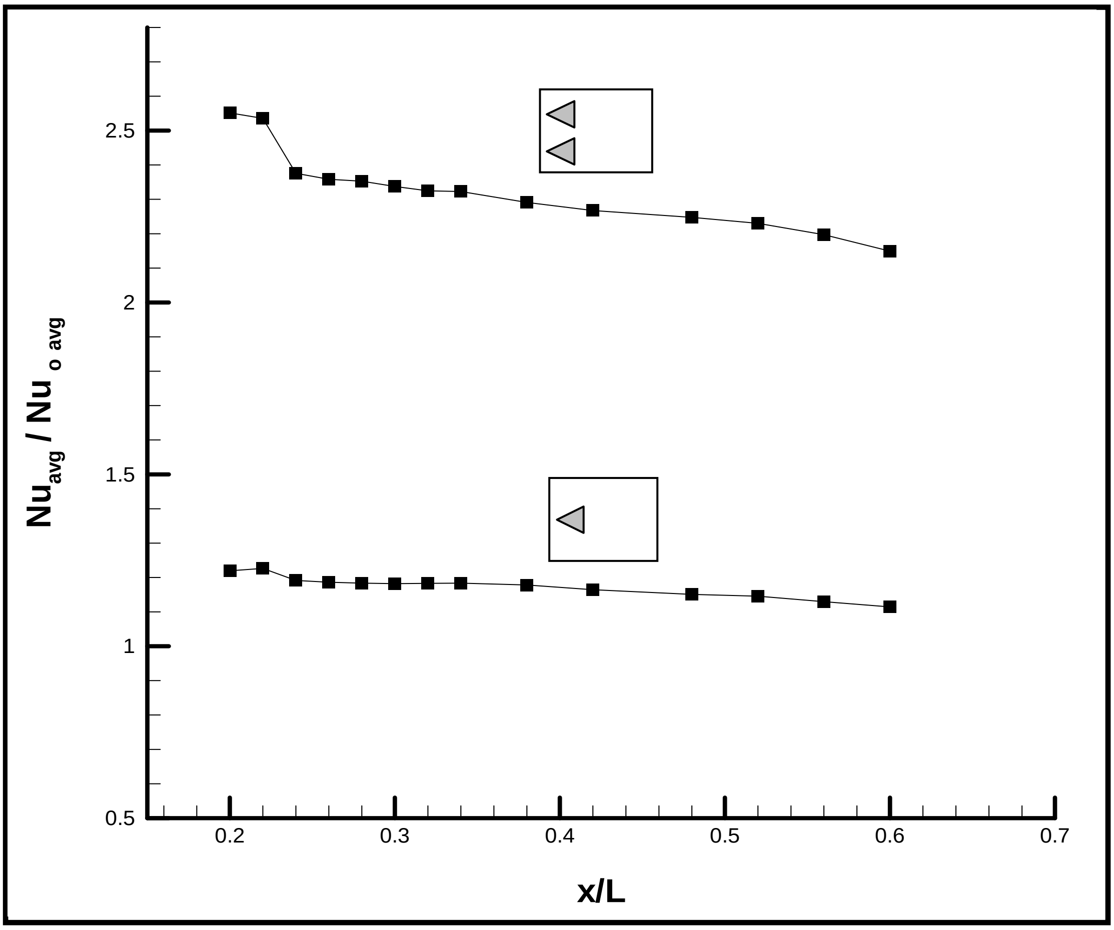

Figure 11: **Spanwise average Nusselt numbers for a single VG and VG pair at Re_H=3712**